Cement and Concrete Research 67 (2015) 310–317

Contents lists available at ScienceDirect

Cement and Concrete Research

journal homepage: http://ees.elsevier.com/CEMCON/default.asp

Contribution of fiber reinforcement in concrete affected by alkali–silica reaction

G. Giaccio [a,c], M.E. Bossio [b,c], M.C. Torrijos [b,c], R. Zerbino [b,c,*]

[a] CIC, Commission of Scientific Research, Department of Civil Engineering, La Plata National University, La Plata, Argentina
[b] CONICET, National Council of Scientific and Technological Research, Department of Civil Engineering, La Plata National University, La Plata, Argentina
[c] LEMIT, 52 e/121 y 122, B1900AYB, La Plata, Pcia. de Buenos Aires, Argentina

ARTICLE INFO

Article history:
Received 23 December 2013
Accepted 27 October 2014

Keywords:
Alkali–aggregate reaction (C)
Degradation (C)
Fiber reinforcement (E)
Mechanical properties (C)
Microcracking (B)

ABSTRACT

Fiber reinforced concrete (FRC) is a high performance material that is frequently used for structures in contact with aggressive environments, because the fibers can control the propagation of cracks. This paper analyzes the residual properties of FRC after the alkali–silica reaction has taken place. The potential contribution of different types of fibers for mitigating the degradation process and their effects on the mechanical and transport residual properties are discussed. The expansions, presence of cracks, compressive strength and modulus of elasticity, and the behavior under flexural loads were evaluated. Steel fibers were the most efficient for reducing the crack density, followed by synthetic macrofibers. The coefficient of air permeability followed the same tendency, showing the positive effect of macrofibers in transport properties. Concretes incorporating steel or synthetic macrofibers conserve their original post-peak loading capacity when severe alkali–silica reaction damage has taken place.

1. Introduction

The incorporation of fibers into concrete controls cracking processes, resulting in great improvements of the material toughness and structures durability. Steel fiber reinforced concrete has been used for decades in tunnels, precast elements, pavements and bridge decks. During the last years many advances in fiber concretes have appeared such as the development of new synthetic and glass macrofibers, the use of self compacting fiber reinforced concretes [1–4], new standards for mechanical characterization tests [5,6] and the introduction of design criteria for fiber reinforced concrete (FRC) in the structural design codes [7].

Although in many cases fibers are incorporated to extend the service life of the structures due to their contribution to control cracking, there exist areas of limited research as the effects of fibers on concrete permeability and porosity or their benefits in the control of diverse degradation processes in concrete. Some studies on cracked FRC under sustained loading show that fibers modify crack patterns, with narrower and closely spaced cracks [8–11]. Other studies related to concrete permeability indicate that fibers reduce internal cracking and improve impermeability [12–14]. It has also been found that as the content of fibers increases, the benefits are greater [15]. On the contrary, some authors have found that fibers increment water and gas permeability [16] while comparing mixes of equal workability.

FRC is frequently used in structures that are in contact with soils or immersed in aggressive environments since the fibers can control the propagation of cracks at both the micro and macro levels. For example, after a year of exposure to a marine environment, FRC shows less severe corrosion than normal concretes, and for cracks of 0.1 mm wide or narrower, the fiber sections remained intact; the corrosion of the steel fibers was not significant being only an esthetic problem and, in addition, improvements in the residual properties of FRC have been found [17,18].

Synthetic microfibers are recommended to prevent cracking and spalling by exposure to fire, nevertheless there is not information about the efficiency of synthetic macrofibers [19–21]. In concretes incorporating steel fibers [22] although concrete stiffness changes due to exposure to high temperatures, fibers still contribute to the residual capacity despite the matrix was severely damaged.

When Alkali–Silica Reaction (ASR) develops the failure mechanism of concrete is clearly affected. Under compressive loads the growth and propagation of matrix cracks tend to start earlier, the ability of aggregates to control cracking decreases and premature failure occurs. In tension, the differences in the crack pattern of sound and damaged concretes are also reflected in the shape of the load deflection curves. Damaged concretes show an increased non-linearity before the peak and a more gradual softening, which indicates that extensive meandering and branching of cracks are taking place [23]. The use of fibers can have a positive economic impact in the construction of dams, to prevent

* Corresponding author at: LEMIT, Commission of Scientific Research, Calle: 52 e/121 y 122, B1900AYB, La Plata, Pcia. de Buenos Aires, Argentina. Tel.: +54 221 4831141/44; fax: +54 221 4250471.
E-mail address: zerbino@ing.unlp.edu.ar (R. Zerbino).

http://dx.doi.org/10.1016/j.cemconres.2014.10.016
0008-8846/

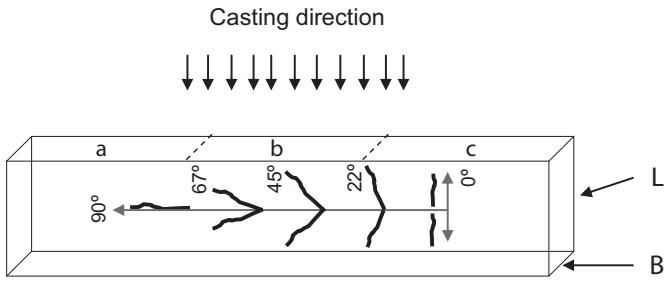

Fig. 1. Scheme of the sectors evaluated for the assessment of crack pattern.

or control the development of deleterious processes [24,25]. Even though fibers could not completely avoid the start of the cracks, they can control their propagation and limit their aperture reducing the permeability and decreasing the degradation rate. It was also found that in the case of ASR, the reductions in the bond capacity of steel or synthetic macrofibers are smaller than the decreases in matrix strength [26].

It is widely recognized that the incorporation of fibers has a positive effect on controlling crack growth, and limiting the crack widths; however, some doubts appear regarding the performance of FRC when suitable conditions for the development of ASR exist. Do fibers change the rate or the total expansions produced by the ASR? Does the type of fiber, steel or synthetic macrofibers, modify the damage produced? Does the use of microfibers modify or control the reaction? After concrete was damaged by ASR, how significant are the changes in the residual capacity (postcracking behavior)?

The main objective of this paper is to analyze the residual properties of FRC after ASR has taken place. The potential contribution of different fibers for mitigating the degradation process and their effects on the mechanical and transport residual properties is discussed.

2. Experiences

FRC with different grades of damage produced by ASR was studied. The expansion over time, presence of cracks, compressive strength and modulus of elasticity, and the behavior under flexural loads were evaluated.

2.1. Materials and mixtures

With the aim of analyzing the effects produced on the residual properties of FRC by the development of ASR, eight concretes with similar mixture proportions (water/cement ratio = 0.42, cement content = 380 kg/m^3) and different alkali contents and fiber types were prepared.

Ordinary Portland cement (Na_2O_{eq} 0.73%), a natural siliceous sand (fineness modulus 2.07) and a 19 mm maximum size granitic crushed stone (fineness modulus 6.91) were used. In addition, to promote the development of ASR, a highly reactive crushed stone (19 mm maximum size, fineness modulus 6.54) was incorporated as a part (40%) of the coarse aggregate. The reactive rock is a quartzitic sandstone, with some chalcedony and opal in the matrix. To obtain plastic concretes, a high range water reducing admixture was used.

Three types of fibers were incorporated: hooked-end steel fibers (S), synthetic macrofibers (M) and synthetic microfibers (m). The S fibers were typical low carbon hooked-end steel fibers, 50 mm in length and 1.00 mm in diameter, with a tensile strength higher than 1100 MPa and an elongation lower than 4%. The M fibers were modified olefin macrofibers with embossed surface, 60 mm in length and 0.62 mm in diameter, 640 MPa tensile strength and a modulus of elasticity of 10 GPa. The m fibers were 12 mm long multifilament polypropylene fibers.

Six fiber concretes named S1, S2, M1, M2, m1 and m2, and two reference concretes without fibers (R1 and R2) were prepared. The concretes were identified according to the type of fiber used. Concretes S1 and S2 incorporated 40 kg/m^3 (0.5% in volume) of steel fibers; concretes M1 and M2 included 3 kg/m^3 of synthetic macrofibers (0.3% in volume) and concretes m1 and m2 contained 1 kg/m^3 of synthetic microfibers (0.1% in volume). These fiber contents were adopted based on the volume of fibers usually incorporated in typical applications of FRC as ground-supported slabs. In concretes R1, S1, M1 and m1 no external alkalis were added and the total alkali content (supplied by the cement) was equal to 2.8 kg/m^3. To enhance the ASR in concretes R2, S2, M2 and m2, NaOH was added in the mixing water to achieve a total alkali equal to 4 kg/m^3. Reference concretes had a slump equal to 100 ± 10 mm and when fibers were incorporated it was reduced to 60 ± 20 mm. The air content was 4 ± 1%.

Table 1
Testing program.

Concrete	Total alkalis (kg/m^3)	Fibers type and content	Age (days)	Expansion (%)	Tests
R1	2.8	None	28	0.009	a, e
			122	0.035	a, e
			380	0.105	a, e
R2	4.0	None	28	0.004	a, e
			168	0.185	b, c, d
			371	0.218	a, e
S1	2.8	40 kg/m^3 hooked-end steel fibers	28	0.006	a, e
			189	0.052	b, c, d, f
			380	0.092	a, e
S2	4.0	40 kg/m^3 hooked-end steel fibers	28	0.011	a, e
			168	0.118	b, c, d, f
			371	0.130	a, e
M1	2.8	3 kg/m^3 synthetic macrofibers	28	0.004	a, e
			167	0.060	b, c, d, f
			380	0.087	a, e
M2	4.0	3 kg/m^3 synthetic macrofibers	28	0.011	a, e
			164	0.182	b, c, d, f
			372	0.190	a, e
m1	2.8	1 kg/m^3 synthetic microfibers	28	0.003	a, e
			168	0.056	b, c, d, f
			380	0.099	a, e
m2	4.0	1 kg/m^3 synthetic microfibers	28	0.010	a, e
			168	0.190	b, c, d, f
			371	0.196	a, e

a: Bending tests (f_L, f_{max}, f_{R1}, f_{R2}, f_{R3}, f_{R4}) — 75 × 105 × 430 mm prisms.
b: Bending tests (f_L, f_{max}, f_{R1}, f_{R2}, f_{R3}, f_{R4}) — 150 × 150 × 600 mm prisms.
c: Crack survey (crack width and crack density) — 150 × 150 × 600 mm prisms.
d: Air permeability — 150 × 150 × 600 mm prisms.
e: Compression tests (f'_c, E) — 100 × 200 mm cylinders.
f: Compression tests (f'_c, E) — 150 × 300 mm cylinders.

2.2. Experimental program and testing methods

Prisms and cylinders were cast with each concrete to be tested at ages between 28 and 370 days. The specimens were compacted by

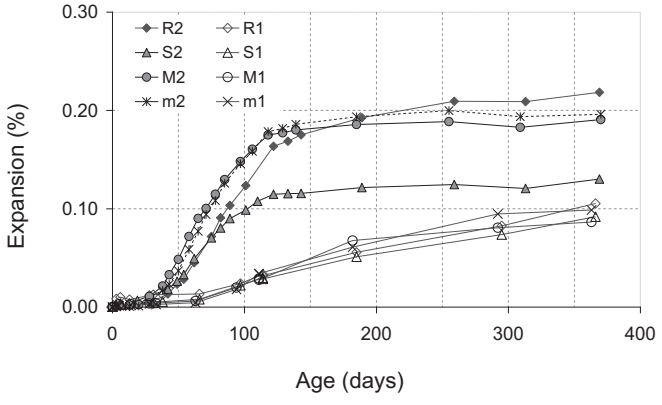

Fig. 2. Linear expansions.

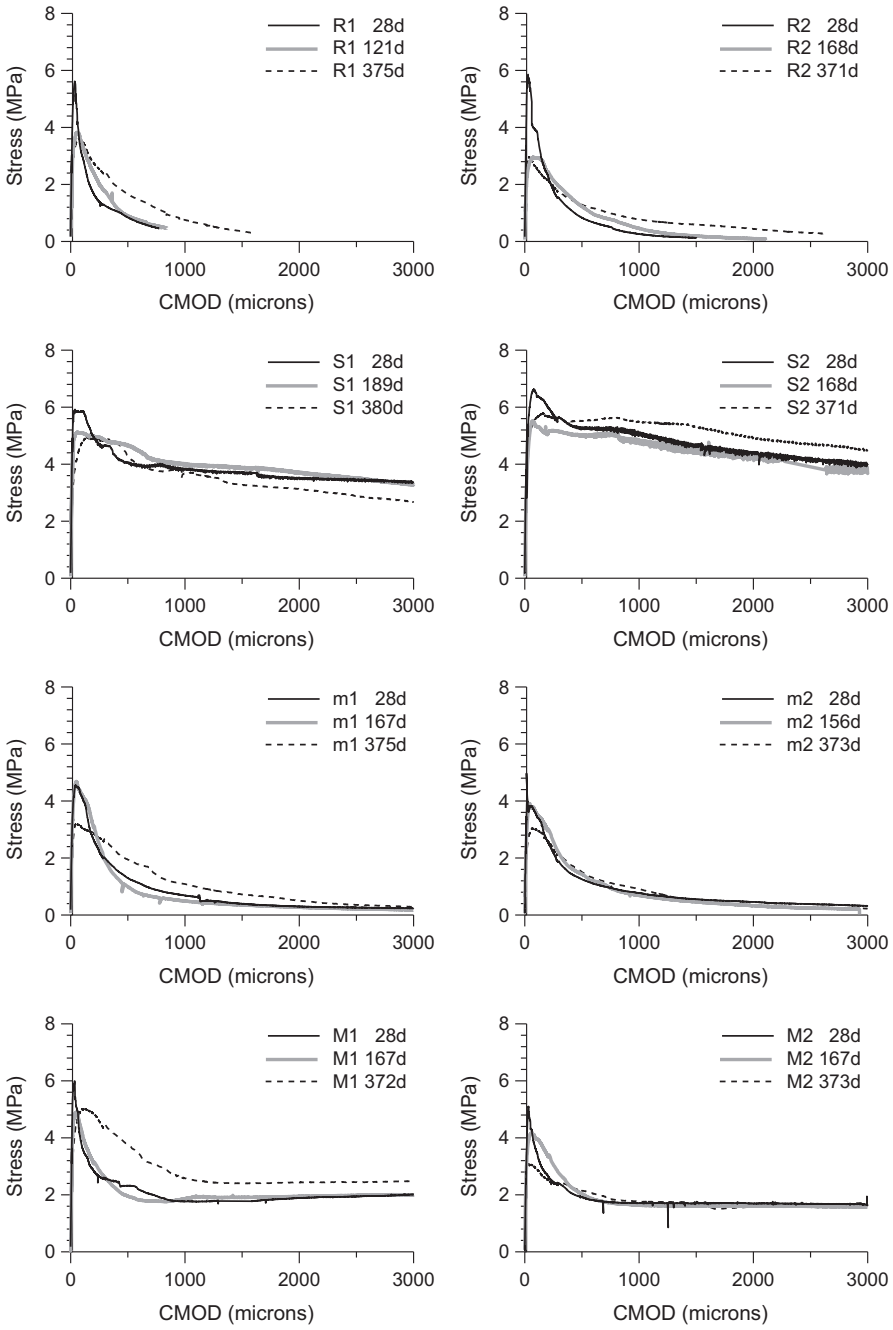

Fig. 3. Stress–CMOD curves at different ages. (To compare similar rotations the CMOD of small beams was corrected by 150 mm/h (mm) [27].)

external vibration and kept protected after casting to avoid water evaporation. After 24 h they were covered with a cotton sheet and placed inside plastic bags including 5 ml of water. These bags were stored in a moist room (20 ± 2 °C, relative humidity > 95%) and, finally, the specimens were tested in saturated condition.

In all concretes, linear expansions were measured as a way to evaluate the ASR process. Expansion measurements were performed on 75 × 105 × 430 mm specimens using a mechanical length comparator with a precision of 0.00254 mm.

Prisms of 75 × 105 × 430 mm and prisms of 150 × 150 × 600 mm were cast to measure the flexural strength and toughness properties in bending. The small prisms, with the same size used to measure expansions, were used to compare the mechanical properties at different ages (different damage levels), while the 150 mm height beams were used to evaluate the crack pattern and the permeability, and to verify the residual mechanical properties. Three point loading flexural tests on notched specimens were carried out in accordance with EN 14651 Standard [5], measuring first-peak strength (f_L), and the residual flexural strengths at 0.5, 1.5, 2.5 and 3.5 mm of crack mouth opening displacement (CMOD), f_{R1}, f_{R2}, f_{R3} and f_{R4}, respectively. The residual flexural strength is a fictitious stress at the tip of the notch which is assumed to act in an uncracked mid-span section, with linear stress distribution [5]. Also, the maximum flexural strength (f_{max}) along the entire postpeak regime was obtained. Tests were performed in a servo-hydraulic testing system through crack width control, using a clip type extensometer. The use of this method with a closed loop control system leads to not only evaluating the residual properties of fiber concrete, but also comparing the postpeak behavior of plain concrete and concrete reinforced with microfibers. To compare the results obtained on beams of different sizes, the length/height and the notch/height ratios remain

Table 2
Bending and compression tests results.

Concrete	Age (days)	Expansion (%)	Bending tests						Compression tests	
			f_L (MPa)	f_{max} (MPa)	f_{R1} (MPa)	f_{R2} (MPa)	f_{R3} (MPa)	f_{R4} (MPa)	f'_c (MPa)	E (GPa)
R1	28	0.009	5.6	5.6	1.0	0.1	–	–	39.2	37.8
	122	0.035	3.6	3.7	1.1	0.3	–	–	41.4	32.3
	380	0.105	3.3	3.4	1.8	0.4	–	–	29.1	25.4
R2	28	0.004	5.7	5.7	0.9	0.1	–	–	35.6	36.4
	168[a]	0.185	2.8	3.0	1.2	0.2	–	–	Not measured	
	371	0.218	2.9	2.9	1.4	0.2	–	–	27.7	24.7
S1	28	0.006	5.6	5.7	3.7	3.3	3.1	2.9	44.1	38.1
	189[a]	0.052	5.0	5.2	4.6	4.4	4.0	3.5	42.3	34.2
	380	0.092	4.8	5.6	4.7	3.5	3.0	2.6	33.9	29.3
S2	28	0.011	6.2	6.4	4.9	4.5	4	3.5	37.9	37.2
	168[a]	0.118	4.7	5.3	4.8	4.6	4.3	3.9	33.7	17.3
	371	0.130	4.7	5.6	5.2	4.7	4.3	3.7	29.1	22.6
M1	28	0.004	6.4	6.4	2.3	1.8	2.0	2.0	38.0	38.0
	167[a]	0.060	5.1	5.1	2.0	1.9	2.0	2.0	40.2	31.9
	380	0.087	4.6	4.8	3.4	2.3	2.3	2.2	32.7	20.0
M2	28	0.011	5.1	5.2	2.3	1.7	1.6	1.6	35.0	35.9
	164[a]	0.182	3.8	3.8	2.1	1.6	1.5	1.5	35.2	21.3
	372	0.190	3.2	3.5	2.2	1.6	1.5	1.5	25.2	20.3
m1	28	0.003	4.6	4.7	1.1	0.4	0.2	0.2	32.7	34.1
	168[a]	0.056	4.8	4.8	0.8	0.3	0.2	0.1	39.9	26.6
	380	0.099	3.1	3.1	2.0	0.7	0.4	0.2	31.1	17.5
m2	28	0.010	4.6	4.7	1.4	0.5	0.3	0.2	33.9	35.0
	168[a]	0.190	3.8	3.9	1.5	0.5	0.1	0.1	33.3	20.1
	371	0.196	2.9	3.0	1.6	0.6	0.3	0.2	24.4	19.1

[a] Big specimens. Prisms 150 × 150 × 600 mm. Cylinders 150 × 300 mm.

constant [27]. Calculating the residual flexural tensile strengths at different CMOD, implies different curvature levels (rotations). In the post-peak region, for a rotation angle ϕ a beam with span length = l and height = h, has CMOD = $h \cdot 2 \cdot \phi$. In prisms with heights h_1 and h_2, for a same rotation ϕ $CMOD_1 = CMOD_2 \cdot (h_1/h_2)$. If the span/height and notch depth/height ratios remain constant, the deformation limits to calculate the residual strengths must be corrected in accordance with the beam height. For instance, the CMOD used to calculate the residual strengths should also be corrected by the factor h (mm)/150 mm. Another easier procedure to calculate the postpeak parameters with the small beams (with the same span/height ratio), is to directly multiply the deformation in the load–CMOD curves by the correction factor 150 mm/h (mm), and then calculate as indicated in the EN standard [27].

To consider the evolution of concrete properties with time, the small specimens were tested at 28 and 370 days approximately. When concretes with high alkali content achieved linear expansions in the order

Table 3
Crack survey and air permeability test results.

Concrete	Face	Air permeability coefficient Kt (10^{-16} m^2)		Cracks characteristics						
				Maximum width (mm)	Mean width (mm)	Density (cm/cm^2)		Orientation (%)		
								0° to 22.5°	45°	67.5° to 90°
R2	B	2.05	2.41	0.10	0.07	0.13	0.19	16	37	47
	L	2.77		0.50	0.23	0.25		26	20	54
S1	B	0.19	0.14	0.05	0.05	0.01	0.01	31	17	52
	L	0.09		0.05	0.05	0.01		23	14	63
S2	B	1.17	1.03	0.10	0.06	0.10	0.10	25	23	52
	L	0.89		0.10	0.07	0.10		23	23	54
M1	B	0.05	0.04	0.00	0.00	0.00	0.01	–	–	–
	L	0.03		0.10	0.10	0.02		14	43	43
M2	B	1.36	1.24	0.10	0.06	0.09	0.11	20	17	63
	L	1.11		0.07	0.05	0.13		17	13	70
m1	B	0.12	0.09	0.08	0.08	0.02	0.02	36	9	55
	L	0.07		0.09	0.08	0.02		37	16	47
m2	B	1.88	2.04	0.10	0.06	0.11	0.15	18	19	63
	L	2.21		0.10	0.06	0.19		10	21	69

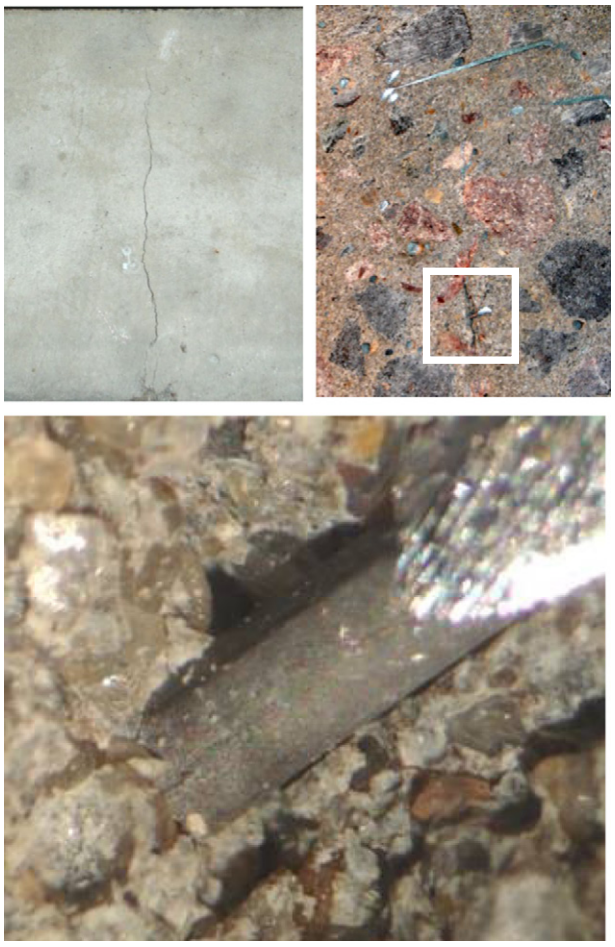

Fig. 4. View of the surface condition of a steel fiber in concrete S2 after two years. Left: Crack on the specimen surface. Right: Cut at 10 mm from the specimen surface. Bottom: detail of a steel fiber that intersects the crack.

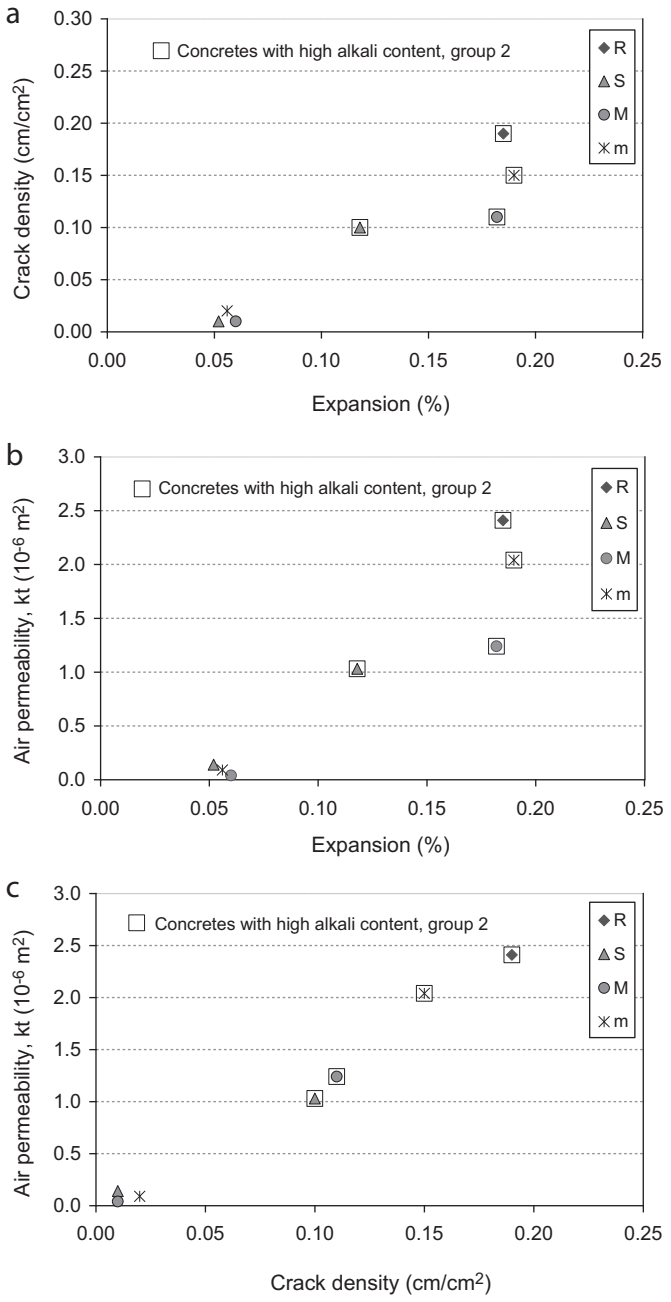

Fig. 5. Relationship between measured properties: a) crack density vs. linear expansion, b) air permeability coefficient vs. linear expansion, c) air permeability coefficient vs. crack density.

of 0.180%, near 6 months old, the larger specimens were tested. In the case of S2 (steel fibers) the tests were performed for a lower expansion.

Before bending tests, the surfaces of the 150 × 150 × 600 mm prisms were carefully examined and the crack pattern was surveyed. Two faces of each prism (the bottom and a lateral face, named B and L respectively) were covered with a transparent film and the surface visible cracks were marked. Each face was divided into three sectors of 150 × 200 mm for a more detailed survey of the crack pattern. The sections were called a, b and c, being a and c the sectors corresponding to the ends of the prisms and b the middle one. The films were scanned, and the obtained images were analyzed with an image-processing software that considers the crack density and orientation. The software measured the length and the angle (maximum Feret angle) of each crack on the image [28]. To define the orientation of cracks, angles of 0, 22.5, 45, 67.5 and 90° were adopted. Fig. 1 shows a scheme of the criterion for the assessment of crack orientations. The crack width was measured with a glass that has a precision equal to 0.05 mm.

In addition to crack pattern evaluation, the damage level was assessed through the measurement of air permeability by Torrent equipment [29,30]. It has a two-chamber vacuum cell and a regulator that balances the pressure in the inner (measuring) and outer chambers. The cell was placed on the surface of the prisms and a vacuum was created with the pump in both chambers. When the inner chamber system is insulated, the pressure in the inner chamber starts to increase, as air is drawn from the underlying concrete. The rate of pressure rise is directly related to the permeability of the concrete. The outer chamber acts as a "guard-ring", creating a controlled, unidirectional air flow into the inner chamber. The equipment gives the coefficient of permeability (kT) calculated on the basis of a theoretical model [31]. The air permeability was measured in the three sectors (a, b, c) on faces B and L of each prism.

Cylinders of 100 × 200 mm were cast with each mix to evaluate the evolution or changes in compressive strength and modulus of elasticity with the development of ASR (tested at 28 days and one year). Cylinders of 150 × 300 mm (a sample size comparable to the width of the beams used to evaluate the crack pattern) were cast to consider the effect of ASR when a higher volume of concrete was involved; they were tested at 6 months. Loading–unloading cycles up to 40% of the maximum stress were applied to determine the modulus of elasticity, then the load was increased monotonically up to failure. Tests and procedures were performed following the general guidelines of ASTM C39 and ASTM C469 standards.

Table 1 summarizes the testing program including the age and the corresponding linear expansion of each concrete, the type of specimen and the tests made.

3. Test results

Fig. 2 shows the linear expansions of the different concretes. As expected, concretes incorporating high alkali content (R2, S2, M2 and m2) showed significant increases in expansion. A high rate of expansion can be seen until near 150 days and then it markedly decreases, achieving in most cases values near 0.2%. Concrete S2, with steel fibers, shows lower expansions; at one year the expansion is near 0.13%. Concretes where no alkalis were added (R1, S1, M1 and m1) show lower expansions, lower rate of expansion (especially at the first ages) and they continue expanding after 150 days. In this case only small differences were observed between the concretes.

Fig. 3 presents the behavior of concretes in tension; typical stress–CMOD curves corresponding to each concrete tested at 28 days and also at near 6 months and one year are shown. In the case of the small beams, in order to consider similar rotations for comparison with the big beams, the represented CMOD was multiplied by the correction factor 150 mm/h (mm). Each concrete shows a different post peak response, in accordance with the type of fiber incorporated. It can be seen that in plain concrete as the damage increases the softening branch of the curves becomes more extended, and they even show some residual load capacity. This behavior is attributed to the possibility of greater branching and meandering of cracks [23]. Similar behavior was found with the microfibers. In concretes with synthetic macrofibers, for both conditions, the loads significantly decrease after achieving the maximum value and they remain almost constant until the end of the test. Finally, steel fiber reinforced concretes present a very gradual descending branch, with high stress values.

The main results from bending and compressive tests are given in Table 2. It includes the first-peak strength (f_L), the maximum flexural strength (f_{max}) and the residual flexural strengths f_{R1}, f_{R2}, f_{R3} and f_{R4} calculated from the stress–CMOD curves as indicated in the EN14651 standard. The residual stresses in prisms of 75 × 105 × 430 mm were calculated with the corrected CMOD in order to consider the same rotations as EN14651 standard beams. In the case of plain concretes or

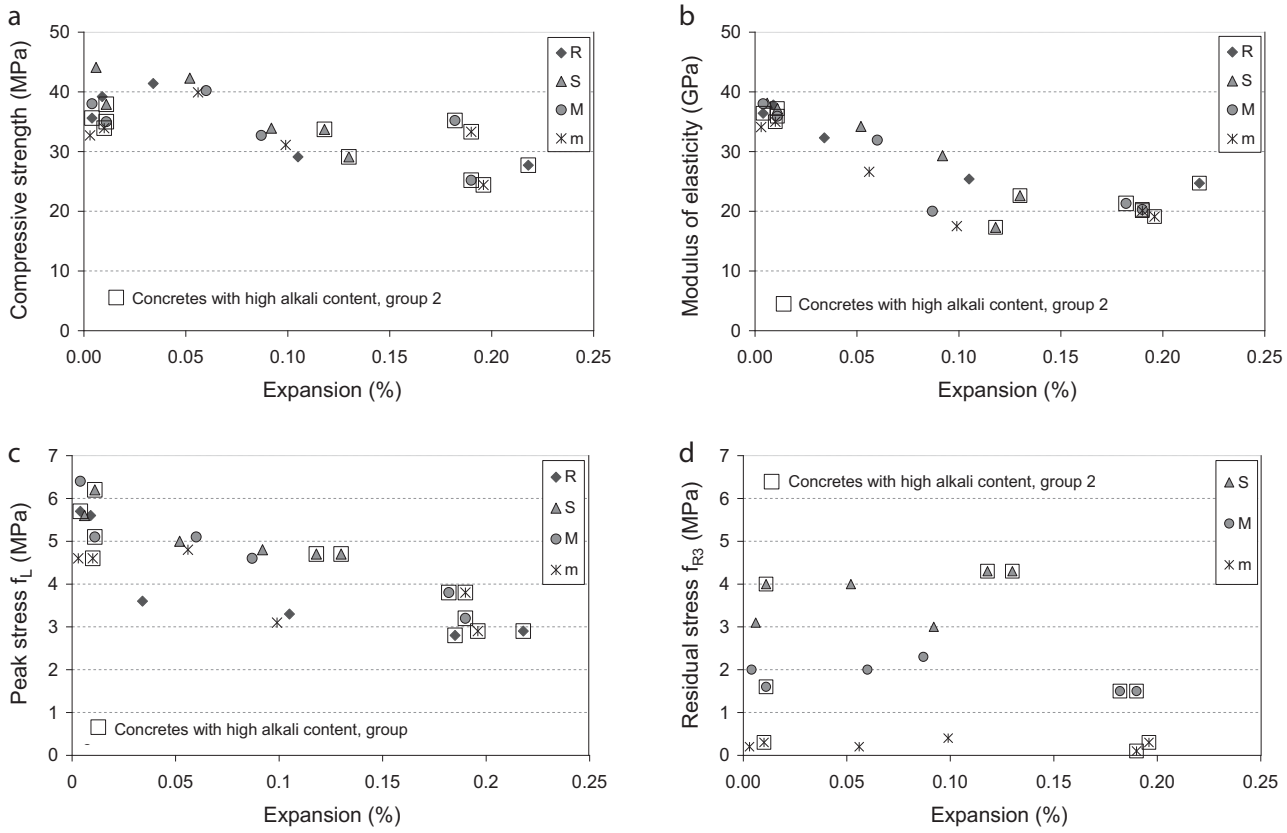

Fig. 6. Relationship between mechanical properties and linear expansions: a) compressive strength, b) modulus of elasticity, c) first-peak strength, d) residual stress corresponding to a CMOD of 2.5 mm (f_{R3}).

concretes incorporating synthetic microfibers (like R or m) the residual strengths are not a parameter of characterization as no residual loading capacity is expected; nevertheless, to compare the behavior of sound and damaged concretes, some values of residual strengths are informed. The compressive strength (f'_c), the modulus of elasticity (E) and the corresponding expansions at the age of testing are also included. It can be seen that as the damage increases the strength and the modulus of elasticity decrease; however in concretes of group 1, where the expansions were smaller, between 28 and 180 days the strength increases and between 6 months and 1 year it decreases. On the contrary, in concretes of group 2, at 6 months the damage is important and the strength is lower than at 28 days. As the modulus of elasticity is more sensitive to the presence of microcracks, in all concretes it decreases with time. Regarding the tensile behavior, it is interesting to note that, in group 2, although the maximum stresses decrease, the residual stress capacity remains almost unaffected in FRC.

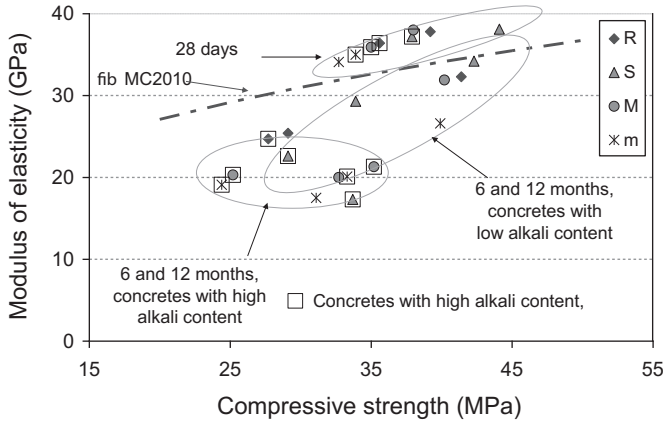

Fig. 7. Relationship between compressive strength and modulus of elasticity.

The results of the crack survey and the permeability tests are given in Table 3. As expected, concretes with higher alkali content showed greater density and size of cracks, with R2 (without fibers) being the most damaged. The same tendency was found in air permeability. Fiber incorporation tends to decrease the quantity and width of the cracks. Steel fibers were the most efficient with a reduction in the crack density of 47% (Concrete S2), followed by concrete with synthetic macrofibers with a 42% less quantity of cracks, while in concrete with microfibers only 21% fewer cracks were found in comparison to concrete R. The variations in air permeability followed the same order, the differences being near 57, 49 and 15% respectively. Table 3 also presents the results of the assessment of cracks orientation, differentiating the percentages of cracks oriented between 0° and 22.5°, near 45° and also between 67.5° and 90°. It can be seen that in all concretes most cracks were orientated along the beam axis (between 67.5° and 90°).

Considering the possibility of corrosion of steel fibers, the surface of the specimens cast with S2 and S1 was examined along the experiences; no signs of corrosion were observed, even in cracked zones. At the age of two years some sections crossing fissures were also analyzed; again, the fibers were sound even those crossing the cracked sections which are in the worst condition. It is important to note that cracks width in these concretes was smaller than 0.1 mm. The results are in accordance with other authors [17] that indicate a small sensitivity of steel SFRC to corrosion, particularly for thin cracks. Fig. 4 shows the aspect of a steel fiber (crossing a fissure) in concrete S2.

4. Discussion

Fig. 5a and b plots the results of the crack density and the air permeability coefficient as a function of the expansion. Concretes S1, M1 and

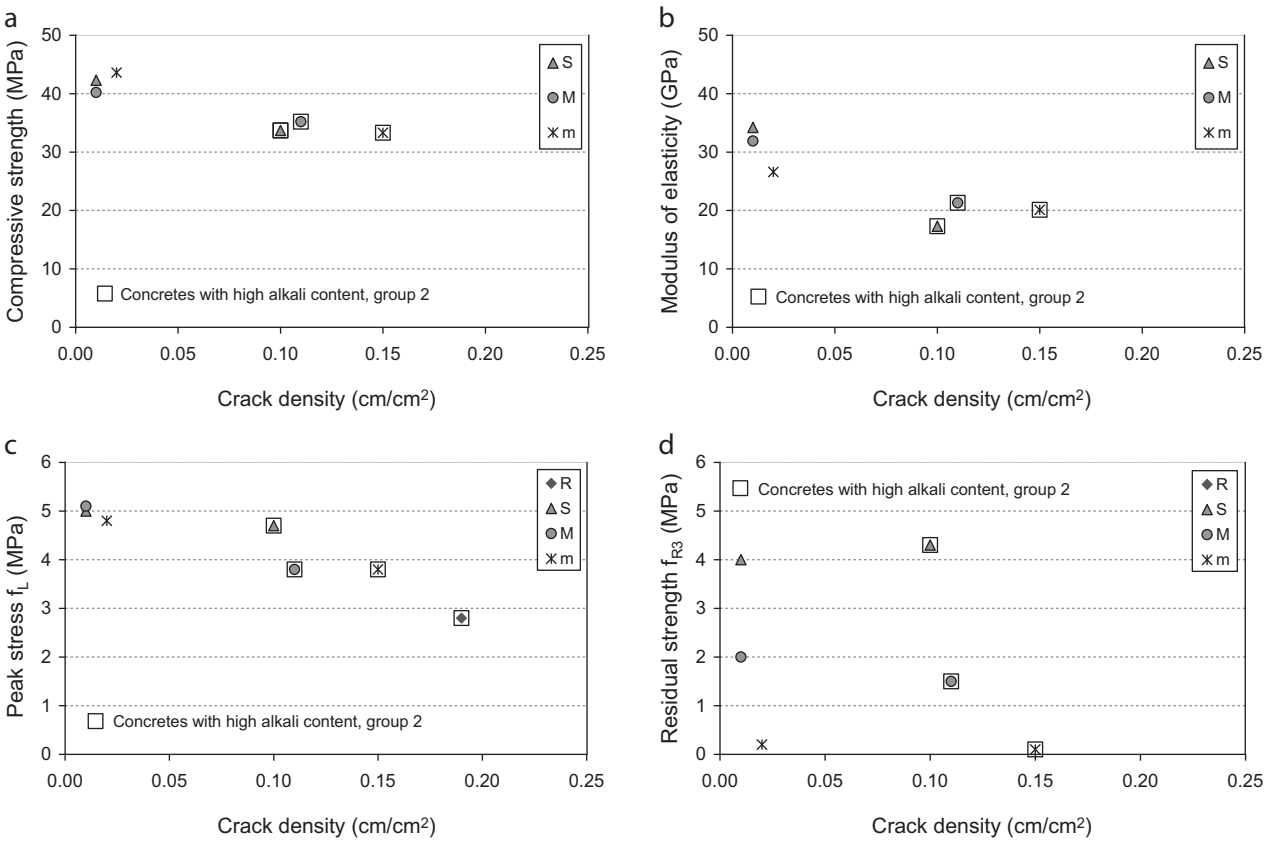

Fig. 8. Effect of cracking on concrete mechanical behavior: a) compressive strength, b) modulus of elasticity, c) first-peak strength, d) residual stress corresponding to a CMOD of 2.5 mm (f_{R3}).

m1, with expansions lower than 0.09%, present very low crack densities with significant increases in group 2. It is interesting to note the different behavior of S2, where the incorporation of steel fibers significantly reduced the expansions, showing the lowest crack density. Concretes R2, M2 and m2, although achieving similar expansions, have different crack densities. The greater values correspond to reference concrete, the crack density was reduced when microfibers were used, and in the case of the synthetic macrofibers although they had higher expansions the crack density was similar to S2. Fig. 5c represents the variation of the coefficient of permeability with the crack density. As expected, there is a very good correlation between these parameters, confirming the positive effect of macrofibers on transport properties. It can be seen that the air permeability grew with the crack density, for densities higher than 0.10 cm/cm^2 the variation was almost linear, while for smaller densities the increase in air permeability was not so marked.

Considering the mechanical properties, Fig. 6 represents the results of compressive strength, modulus of elasticity, first-peak strength (f_L) and the residual strength (f_{R3}) versus the corresponding expansions. As it is known, in damaged concrete the compressive strength and the modulus of elasticity decrease as the deleterious processes advance; the presence of internal cracking leads to greater reductions in stiffness than in strength [23,28]. Fig. 6a and b shows that there is no differentiated response between the plain concrete and the FRC. Fig. 6c plots the variation of first peak strength with the expansions; this parameter is representative of the strength of the matrix. Again the strength decreases as the expansion increases, but in tension, the presence of the macrofibers, particularly the steel ones, improves the behavior of concrete. When the residual stresses are considered a quite different response was found; Fig. 6d, that represents the results of f_{R3} versus the expansions, shows that the residual stress remains almost constant, even for very high expansions. Consequently, FRC incorporating steel or synthetic macrofibers conserves their residual loading capacity when severe ASR damage has taken place. This is in accordance with previous studies that showed minor changes in fiber-matrix bond strength in mortars affected by ASR [26].

Fig. 7 represents the variation of the modulus of elasticity with the compressive strength; it also includes the modulus of elasticity vs compressive strength relationship proposed by the *fib* Model Code 2010 [7]. As it can be seen, when concrete is damaged, the conventional expressions that estimate the modulus of elasticity from the compressive strength are no longer valid. Different zones can be distinguished in the figure: a) tests performed at 28 days (upper-center) where there is less cracking; b) concretes with low alkali content (right) where the modulus of elasticity is lower and increases with the compressive strength and c) the more damaged concretes (center), with high alkali content, with the lowest stiffness.

Finally, Fig. 8 summarizes the effect produced by the cracking developed in each concrete on their mechanical response; the results of compressive strength, modulus of elasticity, first-peak strength (f_L), and the residual strength (f_{R3}) versus the crack density are plotted. It corresponds to the measurements made on 150 mm height beams and 150 mm diameter cylinders at the age of 6 months. Again, the decrease in strength and the remaining values of the residual stresses are the most significant characteristics to highlight.

The present results indicate that although the incorporation of fibers does not avoid ASR, some fibers may be useful to reduce in some extent the expansion rate and magnitude, as well as the induced crack sizes. At the same time, it should be emphasized that, considering their mechanical performance, FRC maintains their residual properties without significant modifications, even when severe matrix damage occurred. Then, the use of FRC is a useful tool to extend the service life of structures as they conserve their residual mechanical properties and crack control capacity even if unexpected significant damage processes take place.

5. Conclusions

This paper evaluates the properties of different types of fibers on the development of ASR cracking and the consequent response of FRC. Hooked-end steel fibers (S), synthetic macrofibers (M) and synthetic microfibers (m) were considered. The main conclusions are shown below:

- Concretes incorporating high alkali contents (R2, S2, M2 and m2) show significant initial rate and magnitude of expansion (near 0.2% at six months); the incorporation of steel fibers (S2) has inhibited the development of the expansions achieving values near 0.13%. In concretes with lower alkali content (R1, S1, M1 and m1), besides the lower values and rate of expansion, only small differences were observed between the different concretes.
- The presence of fibers modified the crack density in concrete. In all cases most cracks were orientated along the beam axis. Concretes with higher alkali content showed greater density and size of cracks, with concrete R2 (without fibers) being the most damaged. Fiber incorporation tends to decrease the quantity and width of the cracks. Steel fibers were the most efficient for the reduction in the crack density, followed by concrete with synthetic macrofibers and concrete with microfibers where fewer cracks than in concrete R were found. The same tendency was found when the coefficient of air permeability was considered, showing the positive effect of macrofibers in transport properties.
- As the damage increases, the compressive strength and the modulus of elasticity decrease, with the modulus of elasticity being the most affected. There were no significant changes produced by the incorporation of fibers when the compressive behavior is concerned.
- Regarding the tensile behavior, a quite different response was found. In FRC the first peak and maximum stresses decrease as the expansion increases; however, the presence of the macrofibers, particularly the steel ones, leads to smaller reductions in strength. On the contrary, and even for very high expansions, the residual stresses remain almost unaffected.

It is very important to highlight that fiber reinforced concretes incorporating steel or synthetic macrofibers conserve their original residual loading capacity when severe ASR damage has taken place.

References

[1] S. Grünewald, J. Walraven, Self-compacting fibre-reinforced concrete, Heron 46 (3) (2001) 201–206.
[2] B. Barragán, R. Zerbino, R. Gettu, M. Soriano, C. de la Cruz, G. Giaccio, M. Bravo, Development and application of steel fiber reinforced self-compacting concrete, Fiber Reinforced Concretes, RILEM PRO 39, BEFIB 2004, ISBN: 2-912143-49-7, 2004, pp. 455–464.
[3] R. Zerbino, J.M. Tobes, M.E. Bossio, G. Giaccio, On the orientation of fibres in structural members fabricated with self compacting fibre reinforced concrete, Cem. Concr. Compos. 34 (2012) 191–200.
[4] L. Vandewalle, G. Heirman, F.V. Rickstal, Fibre orientation in self-compacting fibre reinforced concrete, in: R. Gettu (Ed.), Fiber Reinforced Concrete: Design and Applications, RILEM PRO 60, BEFIB 2008, ISBN: 978-2-35158-064-6, 2008, pp. 719–728.
[5] EN 14651, Test Method for Metallic Fibered Concrete — Measuring the Flexural Tensile Strength (Limit of Proportionality (LOP), Residual), CEN — European Committee for Standardization, Brussels, 2005. 1–17.
[6] ASTM C 1609/C 1609M-07 Standard test method for flexural performance of fiber-reinforced concrete (using beam with third-point loading), ASTM Standards, 2009, Vol. 04.02.
[7] *fib* Model Code 2010, First Complete Draft, International Federation of Structural ConcreteMarch 2010.
[8] E.S. Bernard, Creep of cracked fibre reinforced shotcrete panels, Shotcrete — More Engineering Developments, Taylor & Francis Group, 2004. 47–57.
[9] R. Zerbino, B. Barragán, Long-term behavior of cracked steel fiber reinforced concrete beams under sustained loading, ACI Mater. J. 109 (2) (2012) 215–224.
[10] E. Vasanelli, F. Micelli, M.A. Aiello, G. Plizzari, Long term behaviour of fiber reinforced concrete beams in bending, in: J. Barros (Ed.), RILEM PRO 88, 8th RILEM International Symposium on Fibre Reinforced Concrete: Challenges and Opportunities (BEFIB 2012), Guimaraes, Portugal, ISBN: 978-2-35158-132-2, 2012, pp. 161–162.
[11] G. Tiberti, F. Minelli, G. Plizzari, Crack control in fibrous RC elements, in: J. Barros (Ed.), RILEM PRO 88, 8th RILEM International Symposium on Fibre Reinforced Concrete: Challenges and Opportunities (BEFIB 2012), Guimaraes, Portugal, ISBN: 978-2-35158-132-2, 2012, pp. 187–188.
[12] T. Haktanir, K. Ari, F. Altun, C.D. Atis, O. Karahan, Effects of steel fibers and mineral filler on the water-tightness of concrete pipes, Cem. Concr. Compos. 28 (2006) 811–816.
[13] J.S. Lawler, D. Zampini, S. Shah, Permeability of cracked hybrid fiber reinforced mortar under load, ACI Mater. J. 99 (4) (2002) 379–385.
[14] J. Rapoport, C.M. Aldea, S.P. Shah, B. Ankenman, A.F. Karr, Permeability of Cracked Steel Fiber-Reinforced Concrete, NISS Technical Report Number 115, 2001.
[15] P. Paulík, I. Hudoba, The influence of the amount of fibre reinforcement on the air permeability of high performance concrete, Slovak J. Civ. Eng. 2 (2009) 1–7.
[16] B. Miloud, Permeability and porosity characteristics of steel fiber reinforced concrete, Asian J. Civ. Eng. 6 (4) (2005) 317–330.
[17] J.L. Granju, S.U. Balouch, Corrosion of steel fibre reinforced concrete from the cracks, Cem. Concr. Res. 35 (2005) 572–577.
[18] S.U. Balouch, J.P. Forth, J.L. Granju, Surface corrosion of steel fibre reinforced concrete, Cem. Concr. Res. 40 (2010) 410–414.
[19] S.L. Suhaendi, T. Horiguchi, Effect of short fibers on residual permeability and mechanical properties of hybrid fibre reinforced high strength concrete after heat exposition, Cem. Concr. Res. 36 (2006) 1672–1678.
[20] G.F. Peng, W.W. Yang, J. Zhao, Y.F. Liu, S.H. Bian, L.H. Zhao, Explosive spalling and residual mechanical properties of fiber-toughened high-performance concrete subjected to high temperatures, Cem. Concr. Res. 36 (2006) 723–727.
[21] P. Sukontasukkul, W. Pomchiengpin, S. Songpiriyakij, Post-crack (or post-peak) flexural response and toughness of fiber, Constr. Build. Mater. 24 (2010) 1967–1974.
[22] G. Giaccio, R. Zerbino, Mechanical behaviour of thermally damaged high-strength steel fibre reinforced concrete, Mater. Struct. 38 (2005) 335–342.
[23] G. Giaccio, R. Zerbino, J.M. Ponce, O.R. Batic, Mechanical behavior of concretes damaged by alkali silica reaction, Cem. Concr. Res. 38 (2008) 993–1004.
[24] R.H. Haddad, M.M. Smadi, Role of fibers in controlling unrestrained expansion and arresting cracking in Portland cement concrete undergoing alkali–silica reaction, Cem. Concr. Res. 34 (2004) 103–108.
[25] M.R. Pires de Carvalho, E. de Moraes Rego Fairbairn, R. Dias Toledo Filho, G. Chagas Cordeiro, N.P. Hasparyk, Influence of steel fibers on the development of alkali–aggregate reaction, Cem. Concr. Res. 40 (2010) 598–604.
[26] M.E. Bossio, M.C. Torrijos, R. Zerbino, G. Giaccio, Pull out behaviour of macro synthetic fibres: effects of fibre type, matrix strength and microcracking, in: J.W. Cairns, G. Metelli, G.A. Plizzari (Eds.), Proc. of Bond in Concrete 2012: Bond, Anchorage, Detailing, Fourth International Symposium, Brescia, Italy, Vol 2 — Bond in New Materials and under Severe Conditions, ISBN: 978-88-907078-3-4, 2012, pp. 901–906.
[27] G. Giaccio, J.M. Tobes, R. Zerbino, Use of small beams to obtain design parameters of fibre reinforced concrete, Cement Concr. Compos. 30 (4) (2008) 297–306.
[28] M.C. Torrijos, G. Giaccio, R. Zerbino, Internal cracking and transport properties in damaged concretes, Mater. Struct. 43 (1) (2010) 109–131.
[29] R. Torrent, G. Frenzer, A method for rapid determination of the coefficient of permeability of the "covercrete", International Symposium Nondestructive Testing in Civil Engineering, Proceedings (NDTCE), 1995, pp. 985–992.
[30] R. Torrent, A two chamber vacuum cell for measuring the coefficient of air permeability of the concrete cover on site, Mater. Struct. 25 (1992) 358–365.
[31] M. Romer, Recommendation of RILEM TC 189-NEC: 'Non-destructive evaluation of the concrete cover' comparative test — Part I — Comparative test of 'penetrability' methods, Mater. Struct. 38 (2005) 895–906.